Electronic Supplementary Material (ESI) for Catalysis Science & Technology.

Electronic Supporting Information

Palladium Nanoparticle Deposition on Spherical Carbon Supports for Heterogeneous Catalysis in Continuous Flow

Sarah L. Boyall,[a] Phoebe Berman,[a] Anthony Griffiths,[a] Alexander Massey,[a] Thomas Dixon,[a] Thomas Shaw,[a] Joanna Miller,[a] Jonathan P. White,[a] Robert Menzel,[a] Kevin Leslie,[b] Graeme Clemens,[b] Frans L. Muller,[a] Richard A. Bourne,[a] and Thomas W. Chamberlain*[a]

[a]*Institute of Process Research and Development, School of Chemistry, University of Leeds, Leeds, LS2 9JT*

[b] *Chemical Development, Pharmaceutical Technology & Development, Operations, AstraZeneca, Macclesfield, SK10 2NA, United Kingdom*

*Email: T.W.Chamberlain@leeds.ac.uk; Fax: +44 (0)113 432215

Contents

1. Recirculating Batch Platform

A Knauer Azura P 4.1S dual piston pump (1-10 mL min^{-1}) was used to recirculate the liquid reactants through the column. A Eurotherm temperature controller was used in conjunction with an aluminium heating block to control the temperature of the column (25-250 °C). A Brooks SLA 5800 series MFC (1-300 sscm) was used to control gas flow rate into the equipment. A Diba Omnifit EZ column (6.6 ID, 100 mm in length) was used as the packed bed – packing configuration in section 1. IDEX BPR P-761 and P-763 cartridges (40 and 100 PSI) cartridges were used to control pressure within the system.

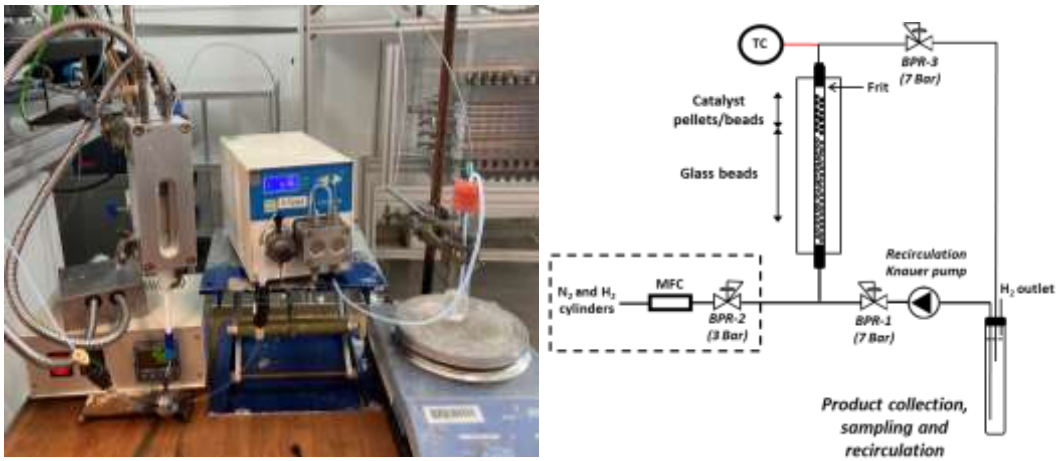

Figure 1 - Image and P&ID of recirculating batch platform.

2. Column Pictures and Description

The column is packed with 2 mm glass beads to increase the mixing of the gas and liquid phases before contact with the catalysts. A layer of 0.5 mm glass beads is then placed on top as they are the same size to the catalyst beads, ensuring the catalyst doesn't fall down the column and stay in a band at the top.

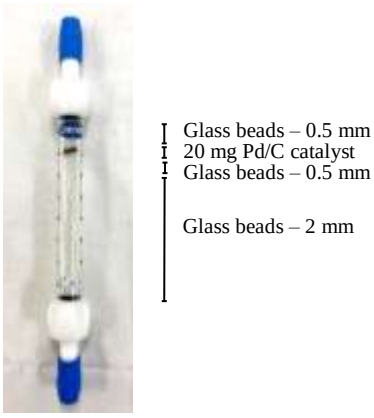

Figure 2 - Packing for Omnifit column with catalyst (20 mg).

3. GC Method Data

Gas chromatography (GC), on an Agilent Technologies 7890B GC System, was used to monitor the reaction as it allows for accurate calculation of the concentrations of analytes. The column used was HP-5 with a temperature range of -60 to 325 ˚C, the column was 30 m in length with a diameter of 0.32 m and film thickness 0.25 µm. The method consisted of an initial hold at 40 °C for 1 minute followed by a temperature ramp to 55 °C over 1 minute. The temperature was then increased to 150 °C over 5.8 minutes and finally ramped to 300 °C over 3 minutes.

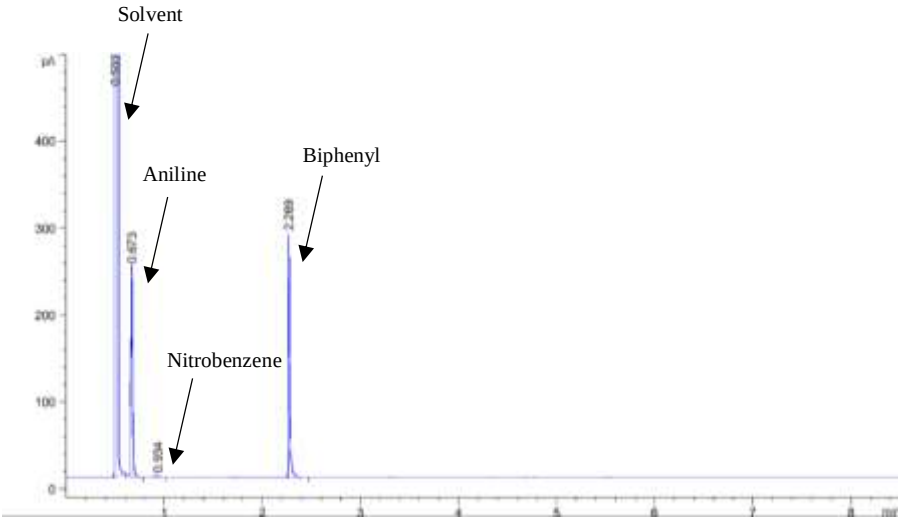

Figure 3 - Example of GC spectra during the reduction of nitrobenzene.

4. Packed Bed Reactor Platform

The reservoir of nitrobenzene and biphenyl was pumped into the reactor with a Knauer Azura P 4.1S dual piston pump (0.1-10 mL min^{-1}) and solvent was pumped through with a Jasco PU-980 dual piston pump (0.05-10 mL min^{-1}). A Eurotherm temperature controller was used in conjunction with an aluminium heating block to control the temperature of the column (25-250 °C). Gas flow into the reactor was controlled by a Bronkhorst El-flow Prestige mass flow controller (MFC – 5-100 sscm). Pressure in the reactor was controlled via a JASCO BP-2080 plus back pressure regulator (BPR – 1-100 bar). Consistent flow from the piston pumps was ensured by using smaller IDEX BPR P-762 cartridges (75 PSI). All fittings, connections and tubing were purchased from Swagelok. Pressure relief valves (RLS series) and inline particulate filters (SS-4TF-2) were purchased from Swagelok and the relief valves were set to 50 bar. An Agilent 1100 HPLC with a VWD or a HP 6890 plus series GC with FID could be connected to the system for online sampling via a Vici EUHA-CI4W.1 sampling valve.

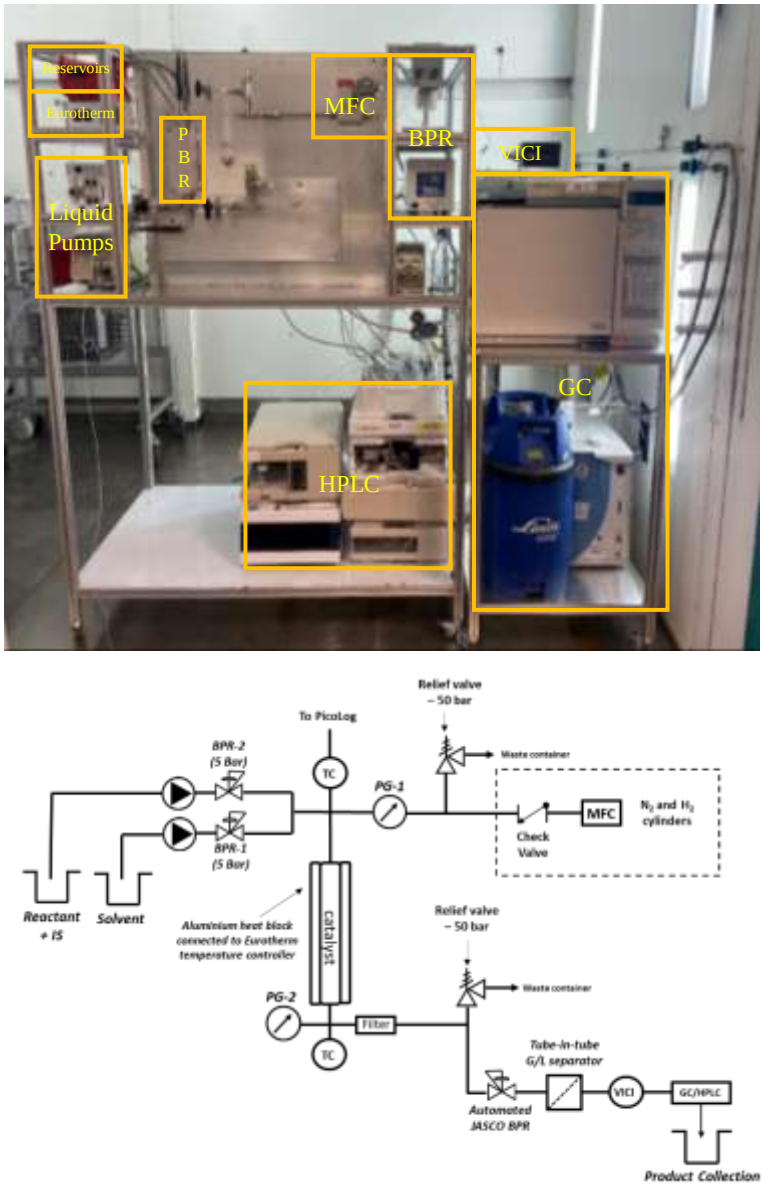

Figure 4 – Image (top) and piping and instrumentation diagram (P&ID) of packed bed reactor (PBR) platform (bottom).

5. Carbon Bead Mastersizer Results

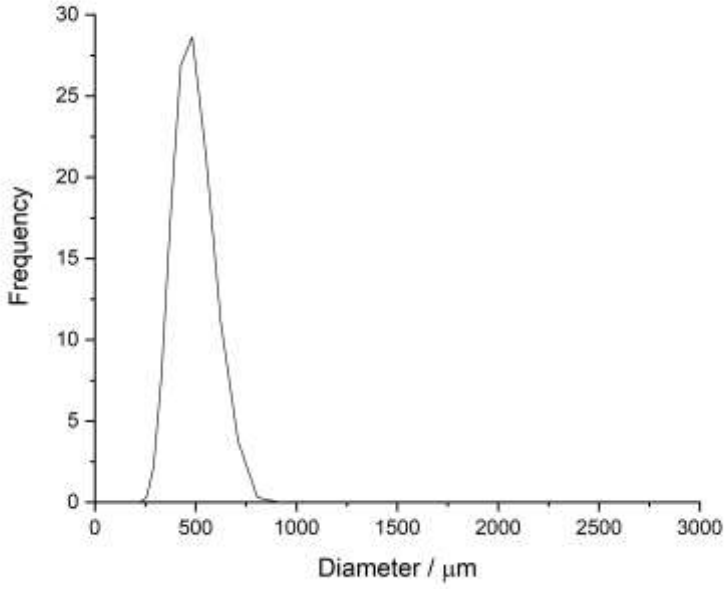

Figure 5 - Mastersizer data showing the average size distribution of the unfunctionalized carbon beads.

6. Summary of BET Data

Table 1 - Summary of BET data for all catalysts.

Catalyst	BJH Ads Pore Volume	BET Surface Area	BJH Ads Average Pore Diameter / nm
1a	0.57	1269.9	16.69
1b	0.74	1295.2	19.61
1c	0.62	1144.1	18.37
1d	0.54	1129.7	16.12
1e	0.60	1136.2	17.30
2a	0.62	1529.9	15.18
2b	0.58	1418.8	16.34
2c	0.56	1242.7	18.86
2d	0.53	1208.7	16.33
2e	0.68	1275.4	20.66
PBSAC beads	0.66	1563.3	15.15
1% Pd/C pellets	0.16	1102.1	3.92
Carbon pellets	0.09	954.4	4.40

7. SEM of Unfunctionalised PBSAC Beads

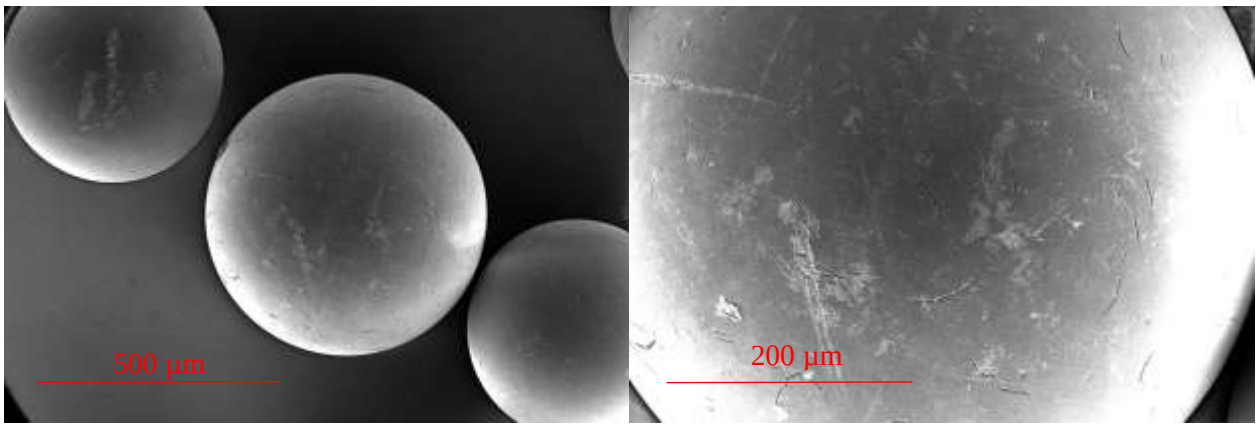

Figure 6 - SEM images of the outer surface of the unfunctionalized carbon beads showing defects and cracks.

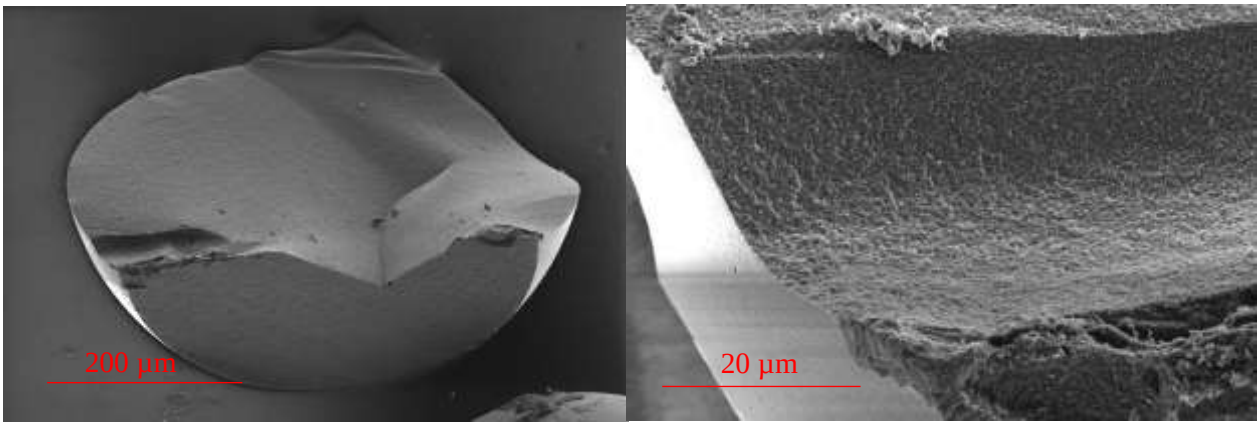

Figure 7 - SEM images of the inner pore network of an unfunctionalized carbon bead that had been cracked open.

8. EDS of Functionalised PBSAC Catalyst

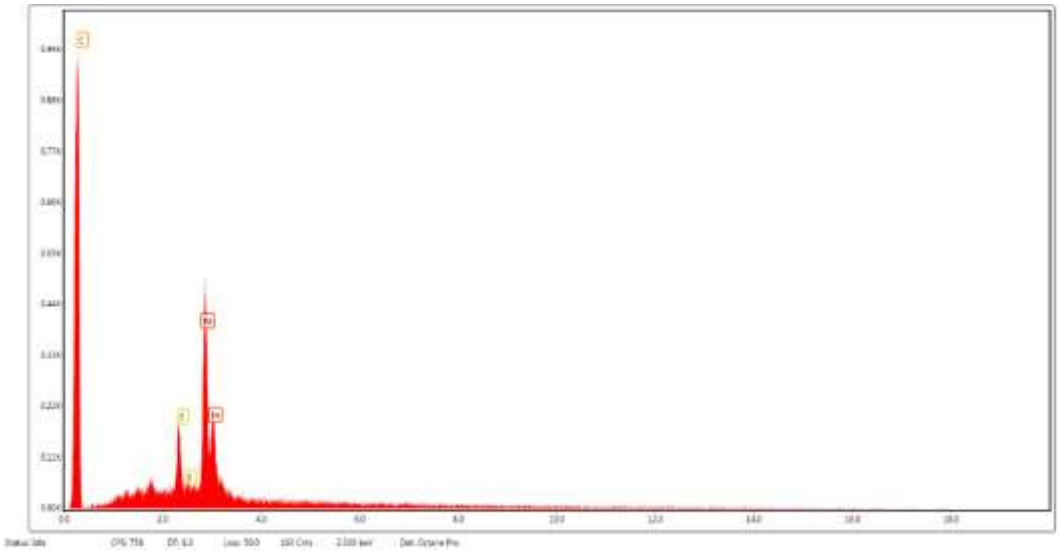

Figure 8 - EDX spectra taken of the outer surface of 1a, showing C and S present from the carbon beads, and Pd from PdNPs.

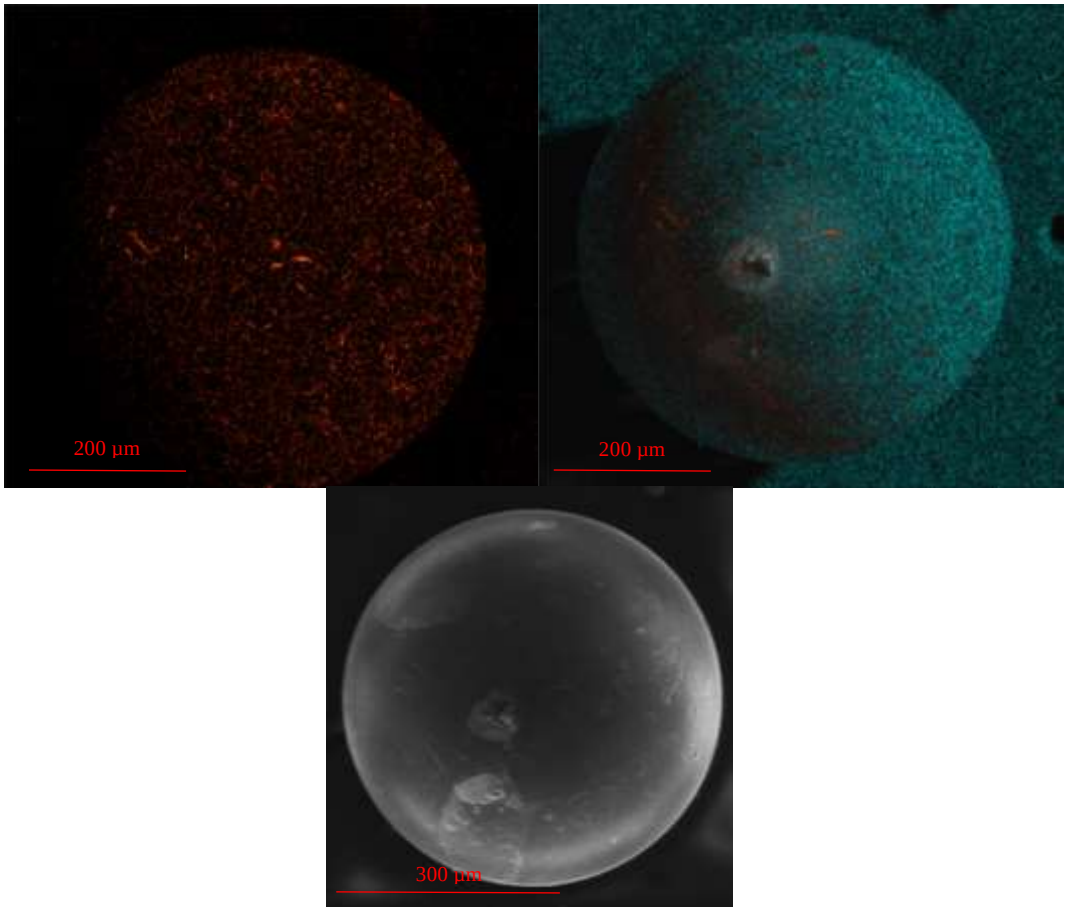

Figure 9 - EDX map and SEM image of catalyst 1a. a) EDX of Pd on carbon bead - red, b) combined EDX of C – blue and Pd -red elements, and c) SEM image of 1a.

9. TEM Images of PBSAC Catalysts

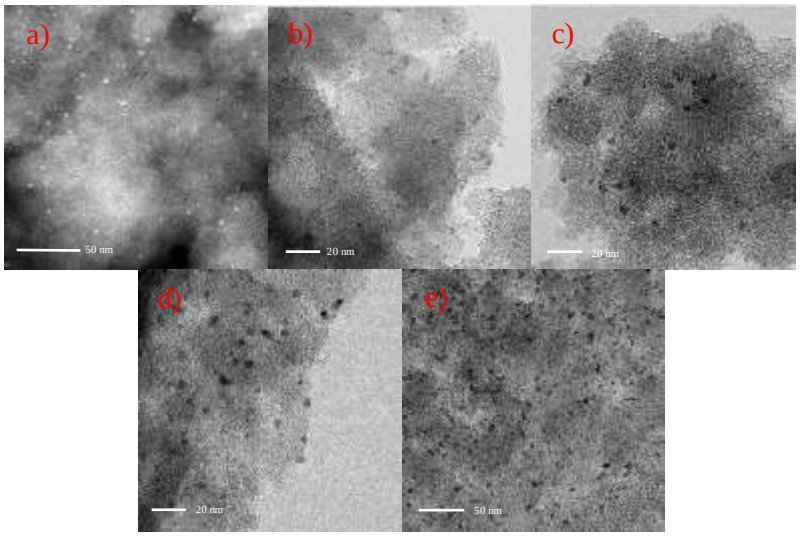

Figure 10 - TEM images for 1a-e.

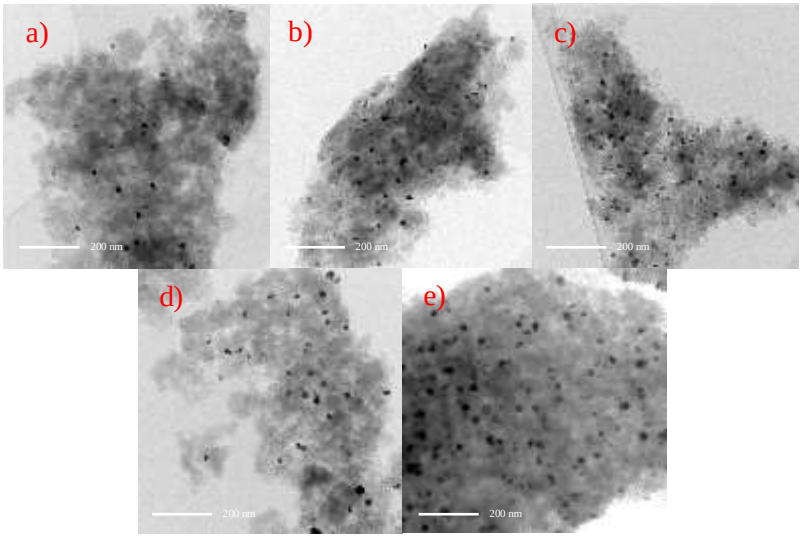

Figure 11 - TEM images for 2a-e.

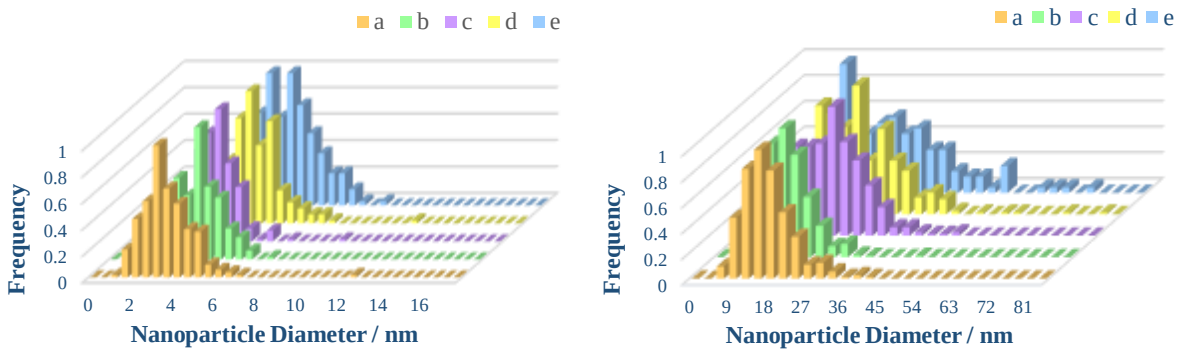

Figure 13 - TEM data showing the size of Pd nanoparticles for different Pd wt.% loadings for 1a-e (left) and 2a-e (right) showing the increase in the average size and size distribution of the PdNPs made via the two deposition techniques (different scales for nanoparticle diameter are used to show the details in more depth).

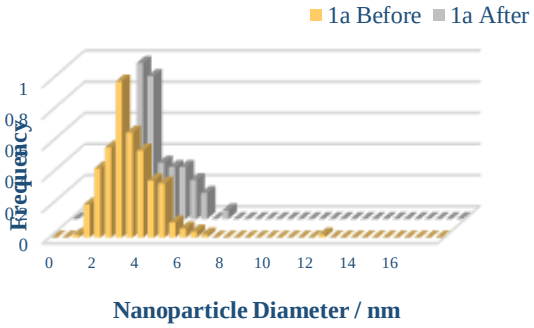

Figure 12 - TEM data showing the difference in size of the 1a catalyst Pd nanoparticles before and after an 11-hour stability test.

10. Plasma FIB-SEM-EDS

Carbon Beads

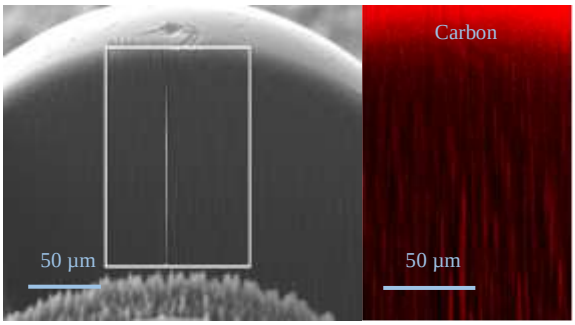

Figure 14 - SEM image and EDS map of unfunctionalised carbon beads.

2e

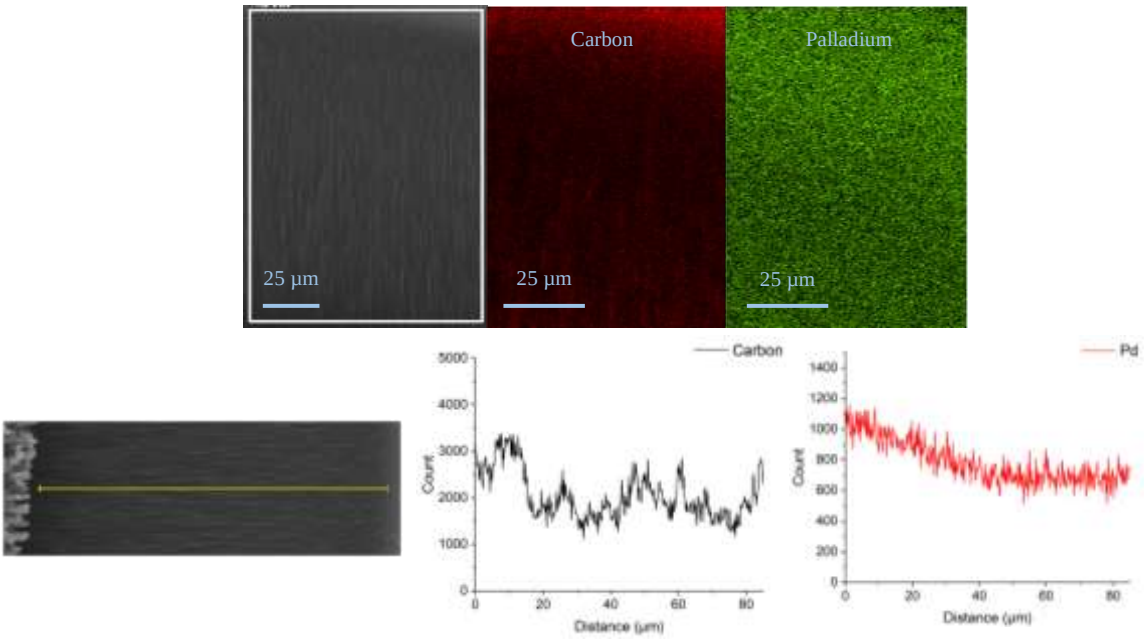

Figure 15 - SEM image, EDS maps and line scans for carbon and palladium elemental content for 2e.

11. Pressure Drop

Pressure drop data was measured for both the 1% Pd/C JM pellets and carbon beads catalyst supports. Pressure transducers were placed either side of the catalyst bed and the reactor was pressurised to 2 bar. The signal from both pressure transducers was recorded and plotted for comparison.

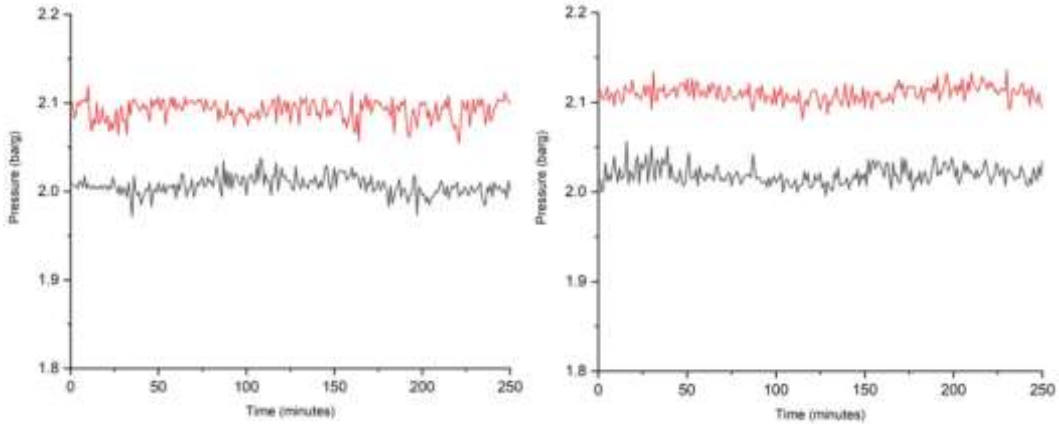

Figure 16 - Pressure drop data, Red = top pressure transducer, black = bottom pressure transducer, Pellets – left, carbon beads – right

12. JM 1% Pd/C Pellet TEM Data

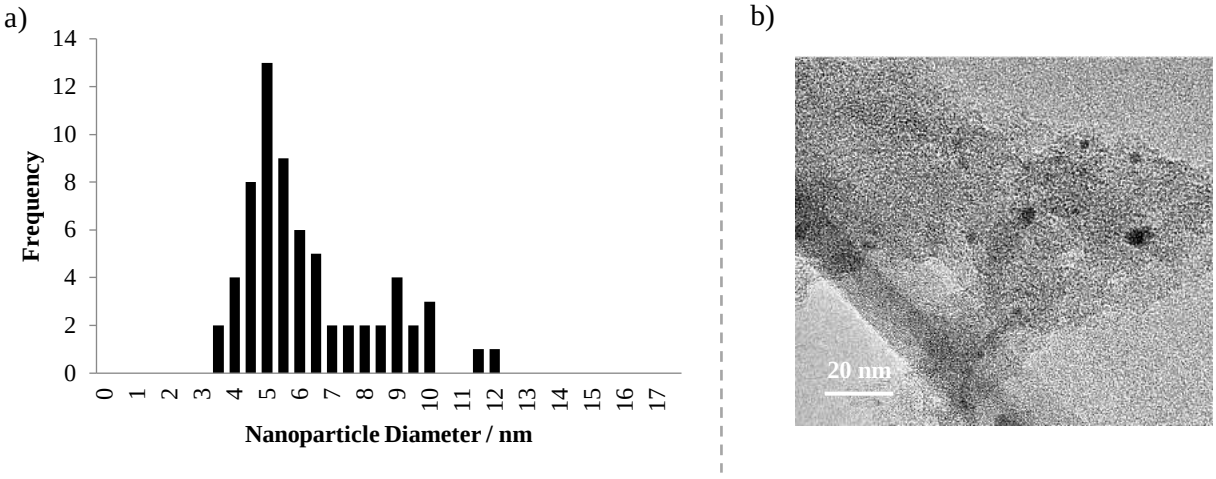

Figure 17 – a) Histogram showing size and size distribution of PdNPs on JM commercial 1 wt.% Pd/C pellets. b) TEM image of PdNPs on commercial pellets.[1]

13. TON and TOF Equations

Turnover numbers (TON) were calculated using Equation 1.

Equation 1: $$TON = \frac{moles\ of\ aniline\ produced}{moles\ of\ Pd\ used\ in\ reaction}$$

Turnover frequency (TOF) was calculated using Equation 2.

Equation 2: $$TOF = \frac{TON}{number\ of\ hours\ of\ reaction\ (hr)}$$

14. Summary of Kinetics and Characterisation Data

Table 2 - Summary of kinetic and characterisation data for catalysts 1a-e, 2a-e and the commercial pelletized catalysts.

Catalyst	Theoretical loading (%)	Actual Loading (%)	Average NP Diameter (nm)	K_{obs} (mol L^{-1} hr^{-1})	TON	TOF (hr^{-1})
1a	1	0.38	3.2 ± 1.2	0.65	2246	374
1b	2	0.60	3.8 ± 1.0	1.41	1553	259
1c	3	1.07	3.7 ± 1.0	0.46	569	95
1d	4	1.32	4.4 ± 1.3	0.88	467	78
1e	5	1.72	5.0 ± 1.4	1.28	346	58
2a	1	0.80	15.3 ± 6.0	0.15	471	79
2b	2	1.08	15.0 ± 5.3	0.13	324	54
2c	3	2.60	18.9 ± 7.8	0.24	194	32
2d	4	3.59	20.7 ± 12.8	0.16	113	19
2e	5	3.81	22.8 ± 13.1	0.22	126	21
Comm	1	1	6.0 ± 2.0	0.30	470	78

15. Literature Rate Data

Table 3 - Rate and TON data collected from literature[2-10].

Catalyst Type	Rate Constant/TON	Reactor Type
10% Pd/carbon paste[2]	TON - 2392	Miniature cascade CSTRs – fReactors – 1.7 mL reactors
Pd-Pt/carbon black[3]	K = 5.5 x 10-3 s^{-1}	STR - Büchi Uster Picoclave reactor – 200 mL
Pd/glassy carbon foam[4]	K = 5.7 x 10-4 s^{-1}	STR - Büchi Uster Picoclave reactor – 200 mL
Pd-maghemite[5]	K = 4.09 x 10^{-2} s^{-1}	STR - Büchi Uster Picoclave reactor – 200 mL
Pd/powdered activated carbon[6]	TOF – 0.26 s^{-1}	STR – Büchi autoclave reactor
Pd nanosheets/layered double hydroxide[7]	TOF = 108.8 hr^{-1}	STR – Autoclave reactor – 7 mL
Au/Zirconia[8]	TOF – 1.58 s^{-1}	STR – Parr autoclave reactor
Immobilised Pt/C coated on capillary tubing[9]	TOF – 1200 h^{-1}	Micro continuous flow reactor
3% Pd/powdered activated carbon [10]	K = 4.5 mol l^{-1} min^{-1}	STR – Parr autoclave reactor – 300 mL

16. Small Scale Packed Bed Reactor for Stability Testing

The recirculating batch platform was adapted, and the outlet of the reactor was moved to a separate reservoir to form a one pass continuous flow system. The set up and operated under the same conditions as run in the recirculating batch platform and samples were taken ever 30 minutes, for the 11-hour stability tests, and every hour for the 24-hour stability test.

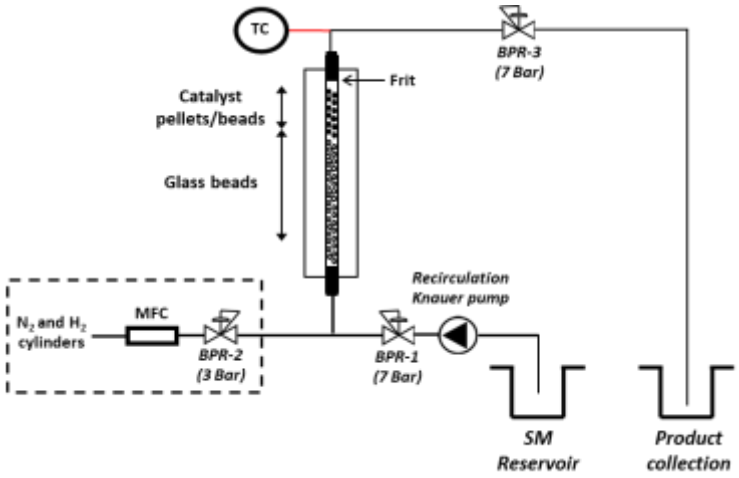

Figure 18 - Small scale continuous flow packed bed reactor for stability testing of small amounts of catalysts.

17. XPS Data

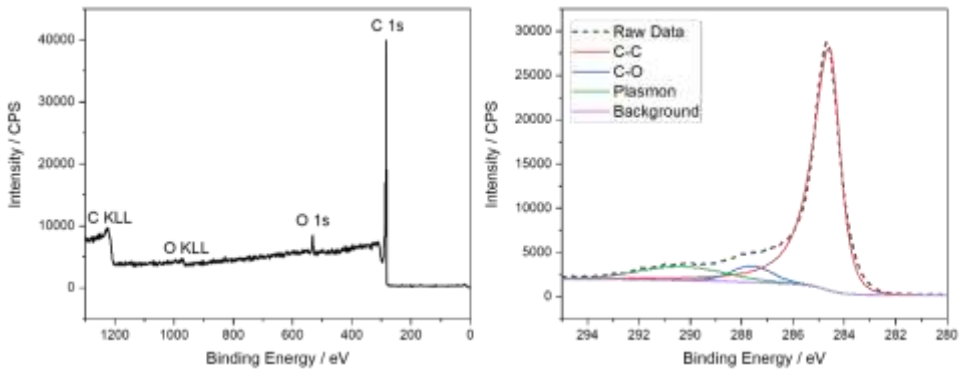

Figure 19 - Survey and high-resolution C 1s spectra for unfunctionalized PBSAC.

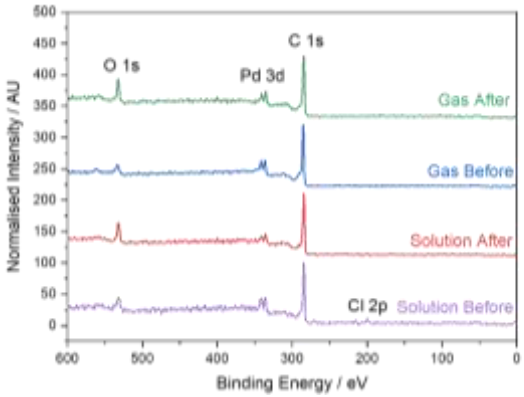

Figure 20 - Survey spectra of 1e (solution) and 2e (gas) prepared by different synthetic approaches, before and after they were used to catalyse the reduction of nitrobenzene.

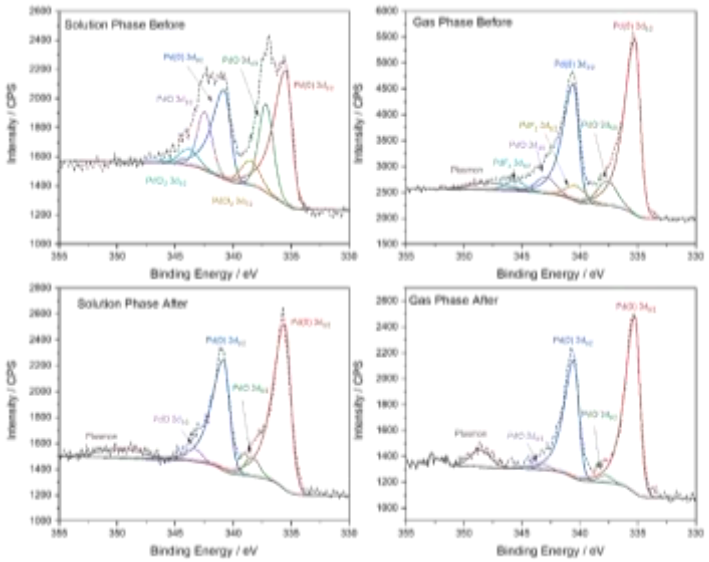

Figure 21 - High-res Pd 3d spectra for the 1e (solution) and 2e (gas) before and after catalysis.

Table 4 - XPS palladium species peak areas and calculated Pd(0):PdO ratios.

Sample	Pd Species	Peak Area (%)	Ratio Pd(0):PdO
1e Before	Pd (0)	61.3	2.1
	PdO	29.8	
	$PdCl_2$	8.9	
1e After	Pd (0)	93.5	14.3
	PdO	6.5	
	$PdCl_2$	0	
2e Before	Pd (0)	79.7	6.4
	PdO	12.4	
	PdF_2	7.9	
2e After	Pd (0)	96.8	30.3
	PdO	3.2	
	PdF_2	0	

18. References

1 J. P. White, PhD Thesis, University of Leeds, 2022.

2 F. Guan, N. Kapur, L. Sim, C. J. Taylor, J. Wen, X. Zhang and A. J. Blacker, *React. Chem. Eng.*, 2020, **5**, 1903–1908.

3 Á. Prekob, G. Muránszky, M. Szőri, G. Karacs, F. Kristály, T. Ferenczi, B. Fiser, B. Viskolcz and L. Vanyorek, *Nanotechnology*, 2021, **32**, DOI: 10.1088/1361-6528/ac137d.

4 Á. Prekob, M. Udayakumar, G. Karacs, F. Kristály, G. Muránszky, A. K. Leskó, Z. Németh, B. Viskolcz and L. Vanyorek, *Nanomaterials*, 2021, **11**, DOI: 10.3390/nano11051172.

5 V. Hajdu, Á. Prekob, G. Muránszky, I. Kocserha, Z. Kónya, B. Fiser, B. Viskolcz and L. Vanyorek, *React. Kinet., Mech. Catal.*, 2020, **129**, 107–116.

6 E. A. Gelder, S. D. Jackson and C. M. Lok, *Catal. Lett.*, 2002, **84**, 205–208.

7 J. Wang, C. Du, Q. Wei and W. Shen, *Energy Fuels*, 2021, **35**, 4358–4366.

8 S. Gómez, C. Torres, J. L. G. Fierro, C. R. Apesteguía and P. Reyes, *J. Chil. Chem. Soc.*, 2012, **57**, 1194–1198.

9 S. Kataoka, Y. Takeuchi, A. Harada, T. Takagi, Y. Takenaka, N. Fukaya, H. Yasuda, T. Ohmori and A. Endo, *Appl. Catal. A Gen.*, 2012, **427–428**, 119–124.

10 M. Turáková, T. Salmi, K. Eränen, J. Wärnå, D. Y. Murzin and M. Králik, *Appl. Catal. A Gen.*, 2015, **499**, 66–76.